

1-1-2017

## Improvement of electrochemical and structural properties of polycarbazole by simultaneous electrodeposition of chitosan

DİDEM BALUN KAYAN

VEYSEL POLAT

Follow this and additional works at: <https://journals.tubitak.gov.tr/chem>

 Part of the [Chemistry Commons](#)

---

### Recommended Citation

KAYAN, DİDEM BALUN and POLAT, VEYSEL (2017) "Improvement of electrochemical and structural properties of polycarbazole by simultaneous electrodeposition of chitosan," *Turkish Journal of Chemistry*. Vol. 41: No. 2, Article 6. <https://doi.org/10.3906/kim-1604-95>  
Available at: <https://journals.tubitak.gov.tr/chem/vol41/iss2/6>

This Article is brought to you for free and open access by TÜBİTAK Academic Journals. It has been accepted for inclusion in Turkish Journal of Chemistry by an authorized editor of TÜBİTAK Academic Journals. For more information, please contact [academic.publications@tubitak.gov.tr](mailto:academic.publications@tubitak.gov.tr).

## Improvement of electrochemical and structural properties of polycarbazole by simultaneous electrodeposition of chitosan

Didem BALUN KAYAN<sup>1,\*</sup>, Veysel POLAT<sup>2</sup>

<sup>1</sup>Department of Chemistry, Faculty of Science and Arts, Aksaray University, Aksaray, Turkey

<sup>2</sup>Osmangazi Anatolian High School, Aksaray, Turkey

Received: 30.04.2016

Accepted/Published Online: 10.09.2016

Final Version: 19.04.2017

**Abstract:** Polycarbazole/chitosan composite materials were synthesized electrochemically at various loadings of chitosan (Chi). Their electrochemical, structural, thermal, and morphological characterizations were investigated by cyclic voltammetry, chronoamperometry, electrochemical impedance spectroscopy, Fourier transform infrared spectroscopy, thermal gravimetry, and scanning electron microscopy. Further electrical conductivity was measured using a four-point probe technique. The electrochemical results showed that the electrical conductivity of the polymeric composite film was increased by increasing the amount of Chi in the electrolyte medium. The as-prepared composite films exhibited enhanced electrical conductivity and structural properties of polycarbazole due to the presence of Chi in the composite films.

**Key words:** Polycarbazole, chitosan, conducting composite, electropolymerization, electrical properties

### 1. Introduction

Polycarbazole is a well-known conducting polymer that has been employed in several applications, such as light emitting diodes,<sup>1,2</sup> electrochromic displays,<sup>3,4</sup> field effect transistors,<sup>5</sup> and modified electrodes.<sup>6–10</sup> Amongst the other conducting polymers, PCz has attracted enormous attention these days due to its good electrical, photoactive properties and deep highest occupied molecular orbital (HOMO) energy level. Polycarbazole and its derivatives are a well-studied class of conducting polymers, but have poor processing abilities due to the  $\pi-\pi$  electron system along their backbone,<sup>7,8</sup> and so it is necessary to prepare mechanically resistant conducting PCz films for practical applications. To further improve their electrical, thermal, and other physicochemical properties, various PCz composites with different components have been synthesized and investigated for potential applications.<sup>8–12</sup> The N–H bond located in the carbazole molecule can be more easily functionalized with other substituents.

On the other hand, chitosan (Chi) is a semicrystalline polysaccharide and quite a unique biopolymer derived from the partial deacetylation of chitin. Due to its excellent film-forming ability, biocompatibility, nontoxicity, high mechanical strength, susceptibility to chemical modifications, and especially low-cost nature, it has been extensively used in various areas, such as in agriculture, medicine, cosmetics, environmental fields, and the food industry. Its low solubility is a disadvantage in practical usages but, nevertheless, various applications of Chi have been reported in the literature.<sup>12–20</sup> Its good film-forming ability has also led to its use in polymeric composites to obtain good mechanical strength and conductive composites. Many attempts have been made to

\*Correspondence: didembalun@aksaray.edu.tr

apply the highly conductive, catalytic, sensor, and mechanical properties of conducting polymers to different practical needs through blending or composite formation. For this purpose, polymeric composites are very attractive for a variety of applications due to many chemical and physical features.

In the present study, PCz/Chi composite films were synthesized for the first time. The electrochemical polymerization was performed in the presence of Chi in an appropriate solvent system for both Chi and carbazole. The purpose of using Chi as a natural polymer in this study was to insert it into the PCz chains and to improve the processability of the PCz composite films.

## 2. Results and discussion

### 2.1. Synthesis of polycarbazole and polycarbazole/chitosan films

The electrochemical syntheses of PCz and PCz/Chi films were performed on a Pt electrode and the schematic illustration of the electrode surface is shown in Figure 1.

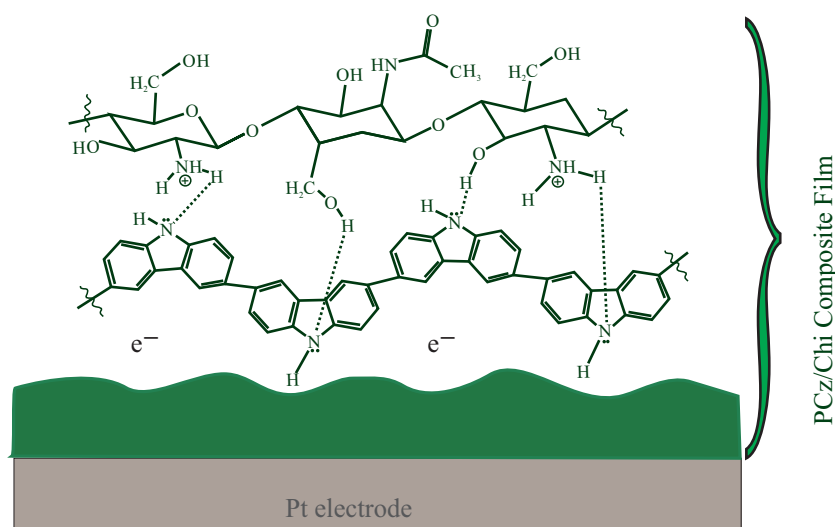


**Figure 1.** Schematic view of the electrode surface.

The polymeric films were achieved successfully by depositing on a Pt disk electrode by cyclic voltammetry after 5 cycles. The recorded cyclic voltammograms of PCz and PCz/Chi films in 0.1 M  $\text{LiClO}_4/\text{ACN}$  as the supporting electrolyte are shown in Figure 2.

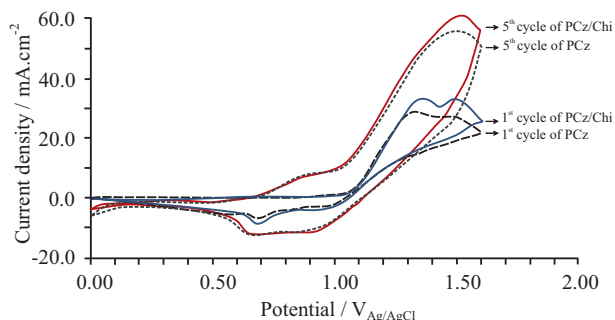


**Figure 2.** The first and fifth cyclic voltammograms of PCz film and PCz/Chi composite film (Composite 1) growing in the 0.05 M Cbz/0.1 M  $\text{LiClO}_4/\text{ACN}$  electrolyte medium ( $\nu = 50$  mV/s).

The optimum film thickness was determined as five cycles. Only the first and fifth cycles of PCz and PCz/Chi films are shown to compare the peak currents. We know from our previous studies that the conductivity of a polymeric film is closely related to its thickness.<sup>21–24</sup> By increasing the number of deposition cycles, depending on the increase in the polymeric film thickness, the heights of the anodic peaks of both the PCz and PCz/Chi films were gradually enhanced, but the PCz/Chi more so, thereby indicating that the presence of Chi increases the current density. Comparing the current density response of the PCz/Chi film with that of the PCz film, it can be seen that the insertion of Chi into the PCz film enhances the current density. This finding indicates that the Chi contributes to electron transfer<sup>13</sup> throughout the polymeric film.

To better understand this behavior, cyclic voltammograms were recorded when there were different amounts of Chi in the electrolyte medium. The observed current density gradually increased with increases in Chi concentration (Figure 3).

An increase in current density was observed by increasing the Chi amount in the electrolyte medium, from Composite 1 to Composite 3. Increasing the concentration of the Chi in the electrolyte medium caused an increase in the current density at the same applied potentials. It can be regarded as proof of the contribution of Chi to electrical conduction in composite structure. The highest amount of Chi in the electrolyte medium for Composite 3 was the maximum concentration that could be added to the electrolyte due to the limited solubility of Chi in this medium.

## 2.2. Chronoamperometric study

Single-step potential chronoamperometry was also employed to investigate the electrochemical behavior of the composite film. In general, the long-term stability of an electrocatalyst during electrochemical processes is a crucial parameter for practical applications. It can be regarded as a valuable electrocatalyst if only the applied current density remains stable as long as possible. Figure 4 shows the chronoamperomogram of the composite film (Composite 3) obtained at the applied potential of +0.8V.

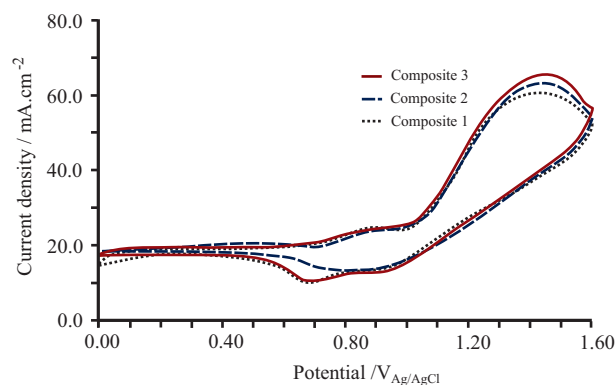


**Figure 3.** The cyclic voltammograms of PCz/Chi composite films in the 0.05 M Cbz/0.1 M LiClO<sub>4</sub>/ACN electrolyte medium ( $\nu = 50$  mV/s).

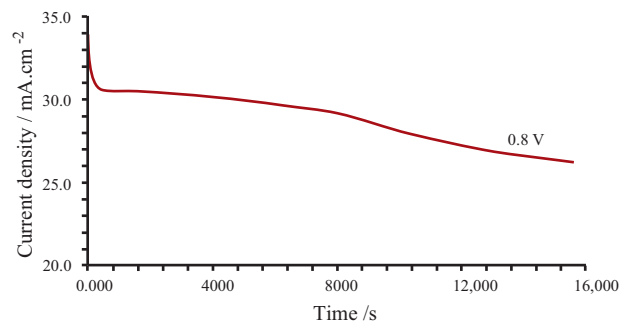


**Figure 4.** The chronoamperometric curve of PCz/Chi composite film (Composite 3) in the 0.1 M LiClO<sub>4</sub>/ACN electrolyte medium.

The obtained current density remained stable for more than 5 h at a current density of 27 mA/cm<sup>2</sup>. This is a good value for PCz films, like other conducting polymers.

### 2.3. Electrical conductivity

It is well known that electrical conductivity is a function of the conjugation length of the polymer. The presence of Chi during electropolymerization helps to increase the conjugation chain length and the free movement of charge carriers.<sup>25–28</sup> Starting from this theory, the electric conductivity of the PCz and PCz/Chi composites were measured and compared, in addition to the electrochemical methods used in this study. The electrical conductivities of the PCz and composite materials are given in the Table.

**Table.** The electrical conductivities of PCz and PCz/Chi composites.

Material	Conductivity (S/cm) $\times 10^{-4}$
Polycarbazole	2.1
Composite 1	3.5
Composite 2	3.9
Composite 3	4.5

As is known, the structural arrangements of the polymer chains might affect the electrical properties of conductive polymers. A higher electrical conductivity was determined for the PCz/Chi compared with the PCz film, indicating that the Chi interacts with PCz chains, and improves the electrical conductivity. The Table shows that there is a good correlation between the amount of Chi in the composites and electrical conductivity. The electrical conductivity of the composite samples increased with an increase in the amount of Chi,<sup>25</sup> and the values lie in the order of  $10^{-4}$  S/cm. These values are in the range of semiconductor conductivities.

### 2.4. Electrochemical impedance spectroscopy studies

Electrochemical impedance spectroscopy (EIS) can provide useful information on the impedance changes of the electrode surface. Lower impedance values indicate higher conductance. Therefore, electrochemical impedance spectroscopy was employed for further investigation in comparing the conductivities of the PCz and PCz/Chi films. The electron-transfer resistance at the electrode surface is equal to the semicircle diameter of the Nyquist plots and can be used to describe the interface properties of the electrode.<sup>29–32</sup> The electrochemical impedance spectra of PCz and composite material films were recorded in a monomer-free solution (0.1 M LiClO<sub>4</sub>/acetonitrile) at open circuit potential in the frequency range of 0.01–100,000 Hz using a Pt disk electrode. The results of the electrochemical impedance are given as Nyquist diagrams in Figure 5.

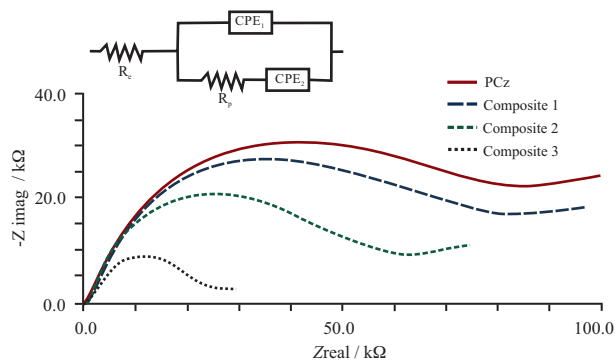


**Figure 5.** The impedance spectra (in Nyquist plot) and equivalent circuit of PCz and PCz/Chi composite films in the 0.1 M LiClO<sub>4</sub>/ACN electrolyte medium.

The Nyquist diagrams for the PCz and the PCz/Chi composites present a semicircle in the high frequency region and a continuous line towards the low frequency region. An electrical equivalent circuit was proposed to fit the system, which includes an electrolyte resistance ( $R_e$ ), polarization resistance or charge transfer resistance at the electrode/solution interface ( $R_p$ ), and constant phase element (CPE) for double layer capacity in real electrochemical cells (CPE<sub>1</sub>: metal/electrolyte double layer capacitance, CPE<sub>2</sub>: polymer film/electrolyte double layer capacitance). It is clearly seen that the diameter of the semicircle ( $R_p$ ) obtained on the PCz film changes with the addition of the chitosan.

As shown in Figure 5, the addition of a small amount of Chi (Composite 1) causes a decrease in the semicircle diameter, which means that the Chi enhances the conductivity of the film by facilitating electron transfer. As the amount of Chi increases more (Composites 2 and 3), the diameter of the semicircle decreases in magnitude more and more as the polymer film becomes more conductive. This decrease indicates that there exists a significant contribution by the Chi amount to the overall conductivity of the polymer film. The results obtained from the electrochemical impedance spectroscopy plots also agreed well with the results of the cyclic voltammetry and conductivity measurements.

## 2.5. Fourier transform infrared spectroscopy (FT-IR) spectra analysis

The FT-IR spectra of the Chi, PCz, and PCz/Chi films (Composite 3) are shown in Figure 6. Chi showed two typical bands at 1664 (carbonyl of amid) and 1592  $\text{cm}^{-1}$  (amino groups).<sup>33</sup> The other bands appearing in the spectrum were due to stretching vibrations of the OH groups in the range from 3750  $\text{cm}^{-1}$  to 3000  $\text{cm}^{-1}$ , which overlapped with the stretching vibration of N-H and C-H bonds.<sup>34</sup> The IR spectrum of PCz had several characteristic bands at 1580  $\text{cm}^{-1}$  (C=C) and 3410  $\text{cm}^{-1}$  (N-H). The following key characteristic bands were observed: 3110–3532  $\text{cm}^{-1}$  (free O-H stretching and N-H stretching with hydrogen bonded secondary amino groups). The composite film illustrated the characteristic peaks of PCz as well as Chi. It is well known that the largest amount of the component in the composites shows the dominant characteristic peaks in the FT-IR spectra. Herein, the characteristic peaks of the PCz are more dominant as it is the larger constituent of the composite than Chi.

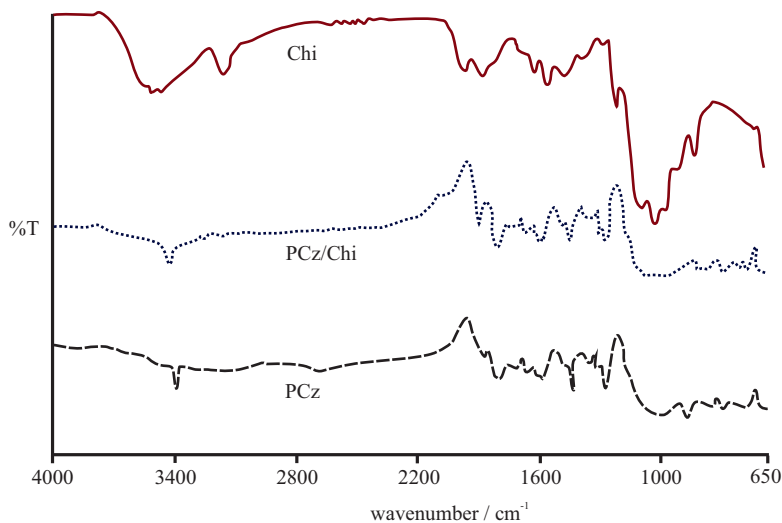


**Figure 6.** The FT-IR spectra of Chi, PCz, and PCz/Chi (Composite 3) composite film.

The aromatic stretching of C=C in the PCz was observed at  $1580\text{ cm}^{-1}$ , but shifted to  $1587\text{ cm}^{-1}$  in the PCz/Chi composite due to the characteristic peaks of  $\text{CONH}_2$  and  $\text{NH}_2$ , as observed in the Chi spectra around  $1600\text{ cm}^{-1}$  and  $1650\text{ cm}^{-1}$ .<sup>35,36</sup> In the spectra of PCz the overlapping peaks of the aromatic ring bending of C–H and perchlorate ion (dopant) were observed at  $1014\text{ cm}^{-1}$ . This peak appears at  $1031\text{ cm}^{-1}$  as a very broad peak in the composite due to C–O–C stretching observed at  $1025\text{ cm}^{-1}$  in the Chi spectra. Furthermore, in the spectrum of the composite a broad absorption band is observed between  $3050$  and  $3350\text{ cm}^{-1}$  due to new hydrogen bonds occurring between the Chi and PCz (shown in Figure 1) in addition to the overlap of the O–H and N–H stretching vibration.

## 2.6. Thermogravimetric analysis

The relative thermal stability of the composite (Composite 3) in comparison with the PCz and the Chi was proved via thermogravimetric analysis (Figure 7). After volatilizing the adsorbed moisture from the structure of the chitosan, one-step decomposition occurs at around  $280\text{ }^\circ\text{C}$ , which could be attributed to the degradation of polymer chains of chitosan.

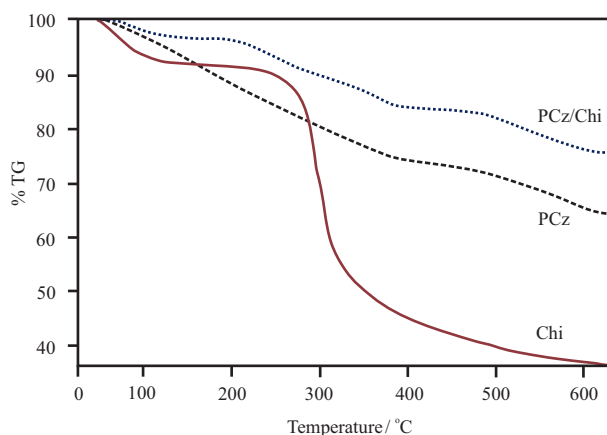


**Figure 7.** The TGA curves of Chi, PCz, and PCz/Chi (Composite 3) composite film.

Figure 7 shows clearly that the peak degradation temperature of the composite was higher than that of pure PCz. The first degradation of the composite occurs between  $30$  and  $130\text{ }^\circ\text{C}$ , and can be explained as the evaporation of volatiles (such as water).<sup>35</sup> The second mass loss appears in the  $250$ – $400\text{ }^\circ\text{C}$  range, which indicates the degradation of dopants, and the most obvious mass loss observed between  $400$  and  $650\text{ }^\circ\text{C}$  consisted of the thermal destruction of the polymer chains. Furthermore, the decomposition rate of the composite was also significantly slower than that of the PCz. Therefore, we can conclude that the thermal stability of the composite was higher than that of the PCz film.

## 2.7. Morphological analysis of surface

For the further characterization of the polymeric composite film, morphological analyses were performed by scanning electron microscopy (SEM). Figure 8 shows the SEM images of the PCz and the resulting product synthesized with Chi (Composite 3).

When the polymerization reaction of PCz was performed without chitosan, the micrograph exhibited the typical structure of the PCz (Figure 8a). However, in the case of the in situ deposition of PCz and Chi, it seems

that the Chi settled into the pores of the PCz and a more uniform, compact film structure was observed (Figure 8b). This uniform structure also provides a better film property and might increase the ability of electron transfer.

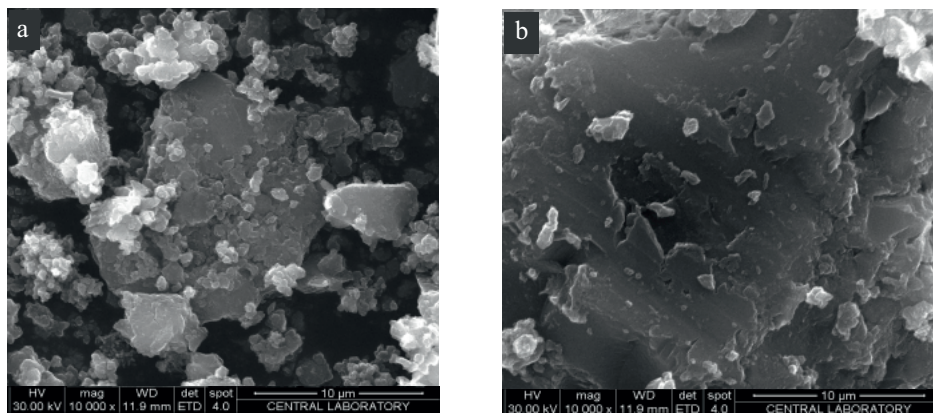


**Figure 8.** SEM images of PCz film (a) and PCz/Chi composite film (b).

A smooth surface of composite film can be a reason for the better electronic conductivity compared to Chi-free PCz film.<sup>37</sup> Therefore, the addition of chitosan has an influence on the structural modification of the resulting product and this is reflected in changes in conductivity as stated in subsection 2.2. Electrical conductivity.

In conclusion, a new conducting composite material has been synthesized electrochemically that possesses both the good electrochemical properties of the PCz and the good film-forming and mechanical properties of the Chi. The interesting part of this study was to obtain mechanically resistant and conductive composites to achieve a synergistic effect in regards to the properties of the two components. Besides the electrochemical, structural, thermal, and morphological studies, the dependence of the electrical conductivity in the composite material with respect to the amount of Chi was examined. The electrical conductivity measurement studies revealed that the composites possessed electrical conductivity in the range of  $10^{-4}$  S/cm.

The results obtained from different measurements confirmed that there existed a certain interaction between PCz and Chi components. Making a composite of PCz film with Chi afforded a visibly better film that peeled easily, provided a significant synergetic effect regarding mechanical properties, and had thermal stability and electrical conductivity. We think that it will induce great interest in carbazole-containing polymers in relation to many industrial applications.

### 3. Experimental

#### 3.1. Reagents and instruments

Carbazole monomer, chitosan (medium molecular weight, 75%–85% deacetylated), acetonitrile (ACN), and lithium perchlorate ( $\text{LiClO}_4$ ) were purchased from Merck without purification. Potentiodynamic, potentiostatic, and impedance spectroscopic measurements were performed using a Gamry Potentiostat (Reference 600) controlled by a personal computer and software (Gamry Framework and Gamry Echem Analyst).



### 3.2. Preparation of polycarbazole and polycarbazole/chitosan composite films

Polycarbazole films were synthesized by cyclic voltammetry in acetonitrile (ACN) solution containing 0.05 M carbazole and 0.1 M lithium perchlorate (supporting electrolyte) and polycarbazole/chitosan composite films were synthesized by addition of chitosan solution to this solution. For electrochemical measurements the polycarbazole and composite films are synthesized on a Pt disk electrode ( $0.0176 \text{ cm}^2$ ) by cyclic voltammetry in the range of 0.0 V to +1.6 V [Ag/AgCl] at a scan rate 50 mV/s in a one-compartment cell equipped with Ag/AgCl (reference electrode) and Pt wire (counter electrode).

For the spectroscopic, thermal, and morphological analyses the polymer and composite films are electrodeposited on a platinum plate ( $6 \text{ cm}^2$ ) to obtain easy peelable thicker films (after 50 cycles by cyclic voltammetry). Another platinum plate with  $6 \text{ cm}^2$  surface area was used as the counter electrode for this experimental setup. The prepared polymer composite films were washed with acetonitrile and distilled water and dried at  $85 \text{ }^\circ\text{C}$  for 24 h.

### 3.3. Preparation of chitosan solution

A stock solution of Chi was prepared by adding Chi (0.01 g) to 10 mL of aqueous acetic acid solution (2%) and stirring for 24 h at  $25 \text{ }^\circ\text{C}$ . Then various amounts of this solution (1 mL -referred to as Composite 1; 2 mL - Composite 2; and 4 mL - Composite 3) were added to a 0.05 M carbazole/0.1 M  $\text{LiClO}_4/\text{ACN}$  electrolyte solution (total 10 mL) to synthesize the polymeric composites.

### 3.4. Electrical conductivity measurements

The electrical conductivities of the samples were measured using a four-point probe technique. The electrodeposited polymers on the Pt plate electrode surface were peeled off carefully and dried at  $85 \text{ }^\circ\text{C}$ , and then the samples were compressed into pellets by a compression-molding machine.

### 3.5. Electrochemical impedance spectroscopy measurements

For the EIS measurements the same experimental arrangement for cyclic voltammetric studies was used, applying a sinusoidal potential of amplitude 10 mV at frequency range from 0.01 to 100,000 Hz.

### 3.6. Spectroscopic analysis

FT-IR spectroscopic analyses were conducted with a PerkinElmer Spectrum 100 FTIR spectrophotometer (in the wavenumber range of  $4000\text{--}625 \text{ cm}^{-1}$ ).

### 3.7. Thermogravimetric analysis

Thermogravimetric analyses of the chitosan, polycarbazole and polycarbazole/chitosan were performed with an EXS – TAR S11 7300 thermal analyzer at a heating rate of  $10 \text{ }^\circ\text{C min}^{-1}$  from  $30$  to  $650 \text{ }^\circ\text{C}$  under nitrogen atmosphere.

### 3.8. Morphological analysis

The surface morphologies of the PCz and PCz/Chi were determined by using a Quanta 400F Field Emission scanning electron microscope.

## Acknowledgments

The authors thank Aksaray University Scientific Research Projects Coordination for their financial support (Project Number: 2012 – 07) and also want to thank Prof Dr Ayfer Menteş for her help with supplying materials.

## References

1. Fu, Y.; Sun, M.; Wu, Y.; Bo, Z.; Ma, D. *J. Polym. Sci., Part A: Polym. Chem.* **2008**, *46*, 1349-1356.
2. Liu, R.; Xiong, Y.; Zeng, W.; Wu, Z.; Du, B.; Yang, W.; Sun, M.; Cao, Y. *Macromol. Chem. Phys.* **2007**, *208*, 1503-1509.
3. Verghese, M. M.; Ram, M. K.; Vardhan, H.; Malhotra, B. D. *Polymer* **1997**, *38*, 1625-1629.
4. Lim, J.; Ko, H. C.; Lee, H. *Synth. Met.* **2006**, *156*, 695-698.
5. Wang, Y.; Hou, L.; Yang, K.; Chen, J.; Wang, F.; Cao, Y. *Macromol. Chem. Phys.* **2005**, *206*, 2190-2198.
6. Moghaddam, R. B.; Pickup, P. G. *Electrochim. Acta* **2013**, *97*, 326-332.
7. Ateş, M. *Mater. Sci. Eng., C* **2013**, *33*, 1853-1859.
8. Joshi, N.; Saxena, V.; Singh, A.; Koiry, S. P.; Debnath, A. K.; Chehimi, M. M.; Aswal, D. K.; Gupta, S. K. *Sens. Actuators B: Chem.* **2014**, *200*, 227-234.
9. Frau, A. F.; Park, Y.; Pernites, R. B.; Advincula, R. C. *Macromol. Mater. Eng.* **2012**, *297*, 875-886.
10. Lei, W.; Wu, Q.; Si, W.; Gu, Z.; Zhang, Y.; Deng, J.; Hao, Q. *Sens. Actuators B: Chem.* **2013**, *183*, 102-109.
11. Yalçinkaya, S.; Demetgül, C.; Timur, M.; Çolak, N. *Carbohydr. Polym.* **2010**, *79*, 908-913.
12. Yalçinkaya, S. *Prog. Org. Coat.* **2013**, *76*, 181-187.
13. Luo, X. L.; Xu, J. J.; Zhang, Q.; Yang, G. J.; Chen, H. Y. *Biosens. Bioelectron.* **2005**, *21*, 190-196.
14. Mostafa, T. B.; Darwish, A. S. *Chem. Eng. J.* **2014**, *243*, 326-339.
15. Abdi, M. M.; Mahmud, H. N. M. E.; Kassim, A.; Yunus, W. M. M.; Mohd, Z. A. T.; Haron, J. *Polym. Sci. Ser. B.* **2010**, *52*, 662-669.
16. He, L.; Wang, H.; Xia, G.; Sun, J.; Song, R. *Appl. Surf. Sci.* **2014**, *314*, 510-515.
17. Cabuk, M.; Alan, Y.; Yavuz, M.; Unal, H. I. *Appl. Surf. Sci.* **2014**, *318*, 168-175.
18. Lu, X.; Qiu, Z.; Wan, Y.; Hub, Z.; Zhao, Y. *Composites Part A: Appl. Sci. Manuf.* **2010**, *41*, 1516-1523.
19. Layek, R. K.; Samanta, S.; Nandi, A. K. *Polymer* **2012**, *53*, 2265-2273.
20. Lee, R. J.; Temmer, R.; Tamm, T.; Aabloo, A.; Kiefer, R. *React. Funct. Polym.* **2013**, *73*, 1072-1077.
21. Köleli, F.; Balun Kayan, D. *J. Electroanal. Chem.* **2010**, *638*, 119-122.
22. Balun Kayan, D.; Köleli, F. *Appl. Catal. B: Environ.* **2016**, *181*, 88-93.
23. Aydın, R.; Öztürk Doğan, H.; Köleli, F. *Appl. Catal. B: Environ.* **2013**, *140-141*, 478-482.
24. Çirimi, D.; Aydın, R.; Köleli, F. *J. Electroanal. Chem.* **2015**, *736*, 101-106.
25. Abdi, M. M.; Kassim, A.; Ekramul Mahmud, H. N. M.; Yunus, W. M. M.; Talib, Z. A.; Sadrolhosseini, A. R. *J. Mater. Sci.* **2009**, *44*, 3682-3686.
26. Li, Y.; Li, G.; Peng, H.; Chen, K. *Polym. Int.* **2011**, *60*, 647-651.
27. Xiang, C.; Li, R.; Adhikari, B.; She, Z.; Li, Y.; Kraatz, H. B. *Talanta* **2015**, *140*, 122-127.
28. Marroquin, J. B.; Rhee, K. Y.; Park, S. J. *Carbohydr. Polym.* **2013**, *92*, 1783-1791.
29. Balun Kayan, D.; Köleli, F. *Turk. J. Chem.* **2015**, *39*, 648-659.
30. Gupta, B.; Singh, A. K.; Prakash, R. *Thin Solid Films* **2010**, *519*, 1016-1019.
31. Ge, S.; Zhang, L.; Zhang, Y.; Liu, H.; Huang, J.; Yan, M.; Yu, J. *Talanta* **2015**, *145*, 12-19.

32. Krushnamurty, K.; Rini, M.; Srikanth, I.; Ghosal, P.; Das, A. P.; Deepa, M.; Subrahmanyam, Ch. *Composites: Part A* **2016**, *80*, 237-243.
33. Ghosh, A.; Ma, L.; Gao, C. *J. Mater. Sci.* **2013**, *48*, 3926-3935.
34. Aneesh, K.; Ravikumar, G.; Berchmans, S. *J. Appl. Electrochem.* **2014**, *44*, 927-934.
35. Kweon, H. Y.; Um I. C.; Park, Y. H. *Polymer* **2001**, *42*, 6651-6656.
36. Tian, F.; Liu, Y.; Hu, K.; Zhao, B. *Polymer* **2004**, *57*, 31-37.
37. Gök, A.; Omastov, M.; Yavuz, A. G. *Synth. Met.* **2007**, *157*, 23-29.